AFRL-SR-AR-TR-03-

0159

REPORT DOCUMENTATION PAGE

1. REPORT DATE (DD-MM-YYYY)	2. REPORT TYPE	3. DATES COVERED (From - To)
22 March 2003	Final	09/30/99-12/31/02

4. TITLE AND SUBTITLE
Controlled Precipitation of Radiation Belt Particles

5a. CONTRACT NUMBER

5b. GRANT NUMBER
F49620-99-1-0339-P00003

5c. PROGRAM ELEMENT NUMBER

6. AUTHOR(S)
Bell, Timothy F.

5d. PROJECT NUMBER

5e. TASK NUMBER

5f. WORK UNIT NUMBER

7. PERFORMING ORGANIZATION NAME(S) AND ADDRESS(ES)

STAR Laboratory
Stanford University
Stanford, California
94305

8. PERFORMING ORGANIZATION REPORT NUMBER

9. SPONSORING / MONITORING AGENCY NAME(S) AND ADDRESS(ES)
Air Force Research Lab.
29 Randolph Road
Hanscom AFB, Maine 01731-
Program Manager: Major P.J. Bellaire, Jr.

10. SPONSOR/MONITOR'S ACRONYM(S)

11. SPONSOR/MONITOR'S REPORT NUMBER(S)

12. DISTRIBUTION / AVAILABILITY STATEMENT
Approved for public release, distribution unlimited

13. SUPPLEMENTARY NOTES

14. ABSTRACT

The overall objectives of this work were to quantify the requirements for controlled precipitation of radiation belt particles in order to mitigate enhanced space particle effects, to address critical issues of antenna-plasma coupling, and to develop a model of the effective radiated power throughout the magnetosphere. In carrying out this effort, Stanford University worked closely with AFRL/VSB. During the period of performance, Stanford University concentrated on the critical issues which determine the properties of the ion and electron sheaths which surround dipole antennas in a plasma. The accurate modeling of the ion and electron sheaths and their effects on the far-field pattern of the antenna is necessary in order to simulate the characteristics of an antenna radiating at ELF/VLF frequencies in the magnetosphere.

15. SUBJECT TERMS
Mitigation of enhanced radiation belt energetic particle fluxes, characteristics of VLF dipole antennas in the radiation belts, energetic electron precipitation

16. SECURITY CLASSIFICATION OF:			17. LIMITATION OF ABSTRACT	18. NUMBER OF PAGES	19a. NAME OF RESPONSIBLE PERSON
a. REPORT	b. ABSTRACT	c. THIS PAGE			Maj. P. J. Bellaire, Jr.
					19b. TELEPHONE NUMBER (include area code)

2311 AX
Received 1 Apr 03
Accepted 3 Apr 03
PJB

FINAL TECHNICAL REPORT

SPONSOR: DEPARTMENT OF THE AIR FORCE

SPONSER REF: F49620-99-1-0339

TITLE: CONTROLLED PRECIPITATION OF RADIATION BELT PARTICLES

Period of Performance: 09/30/99 - 12/31/02

Principle Investigator: Professor U. S. Inan

STAR Laboratory, Stanford University

Report prepared by: Timothy F. Bell
Senior Research Associate
STAR Laboratory, Stanford University
March 24, 2003

SUMMARY

During the period of performance a program of theoretical studies was carried out with the objective of quantifying the requirements for controlled precipitation of radiation belt particles in order to mitigate enhanced space particle effects, to address critical issues of antenna-plasma coupling, and to develop a model of the effective radiated power of both dipole and loop antennas throughout the magnetosphere. In carrying out this effort, Stanford University worked in conjunction with AFRL/VSB scientists. As a result of these studies, Stanford University has developed a model which for the first time quantifies the radiated electromagnetic power in the 1-10 kHz frequency range which is necessary to reduce the lifetimes of energetic electrons in the radiation belts by an order of magnitude. In addition, a method was developed to control the ion and electron sheaths which surround dipole antennas in a plasma. Without such control, the sheath effects strongly diminish the radiation efficiency of dipole antennas, and much larger transmitter power is required to produce the electromagnetic wave fields necessary to control the radiaton belts.

FINAL TECHNICAL REPORT

1. Contract Purpose

The overall purpose of this work was to quantify the requirements for controlled precipitation of radiation belt particles in order to mitigate enhanced space particle effects, to address critical issues of antenna-plasma coupling, and to develop a model of the effective radiated power from dipole antennas throughout the magnetosphere. In carrying out this effort, Stanford University worked closely with AFRL/VSB scientists. Stanford University concentrated on: 1) developing a model to quantify the radiated electromagnetic power in the 1-10 kHz frequency range which is necessary to reduce the lifetimes of energetic electrons in the radiation belts by an order of magnitude, and 2) developing a method to control the ion and electron sheaths which surround dipole antennas in a plasma.

2. Period of Performance

The period of performance under this contract extended from September 30, 1999, through December 31, 2002.

3. Work Provided

During the period of performance of this grant, Stanford University carried out the following tasks:

Task 1: Stanford developing a model to quantify the radiated electromagnetic power in the 1-10 kHz frequency range which is necessary to reduce the lifetimes of energetic electrons in the radiation belts by an order of magnitude.

Task 2: Stanford developed a method to control the ion and electron sheaths which surround dipole antennas in a plasma.

Task 3: Stanford developed a method to calculate the near field and the radiated electromagnetic fields from dipole antennas in the radiation belts.

Task 3: Stanford performed grant management, reporting, and technical overview activities of work.

6. Results of Research Effort

Detailed results of the Stanford research effort are reported in Appendix A.

7. List of personnel contributing to report

The list of Stanford University scientists and engineers who contributed to the work reported in this document is as follows:

Tim Bell

Jacob Bortnik

Tim Chevalier

Umran Inan

APPENDIX A.
Progress Report for AFRL Grant F49620-99-1-0339 Entitled: Controlled Precipitation of Radiation Belt Particles

AFRL Grant F49620-99-1-0339 has been carried out in cooperation with AFRL/VSB. Below in Sections A, B, and C we list the significant accomplishments resulting from work carried out predominantly at Stanford University STAR Laboratory. Joint work with AFRL/VSB personnel is discussed in Section D.

A. Simulation Models.

The first Stanford goal has been the determination of the radiation efficiency and input impedance of dipole antennas in the magnetosphere, including the effects of the plasma sheath surrounding each antenna element. An antenna operating at ELF/VLF frequencies in the magnetosphere will radiate waves with wavelengths of many kilometers. At the same time the sheath surrounding this antenna will have a scale which ranges from centimeters to meters as the antenna voltage is varied. To completely resolve this space from antenna to far field using a fixed cell size of 1 cm in a FDTD simulation would require 100000^3 cells. This requirement is far greater than that which even the most powerful of contemporary supercomputers can satisfy. Thus it is necessary to partition the simulation space into regions in which different scale sizes prevail. As illustrated in Figure 1, we have chosen to partition the simulation space into three separate regions: 1) the plasma sheath region, extending out to a few meters from the antenna, in which either electrons or ions predominate according to the sign of the antenna voltage, and in which these particles are accelerated to high velocities by the quasi-electrostatic fields; 2) the nonlinear warm plasma region, extending from a few meters out to 100 m from the antenna, in which the plasma is essentially neutral but the acceleration due to the electric and magnetic fields produced by the antenna currents is large enough to preclude the use of a linear cold plasma formulation; and 3) the cold plasma region in which the plasma is essentially neutral and particle energization is small.

In order to make progress on this topic we have developed a series of simulation models, each of which applies to one of the regions shown in Figure 1. To date we have tested and verified each model. Our ultimate goal is to combine the simulation models to produce a complete description of the particles and fields within the entire space. The most complicated simulation model is that which applies to region 2, the hot plasma

region. The simulation here involves a 3-D fluid model of the dynamics of electrons and ions under the influence of the electromagnetic and quasi-electrostatic fields produced by the currents and charges on the dipole antennas. We discuss this model first below. The other models are described thereafter.

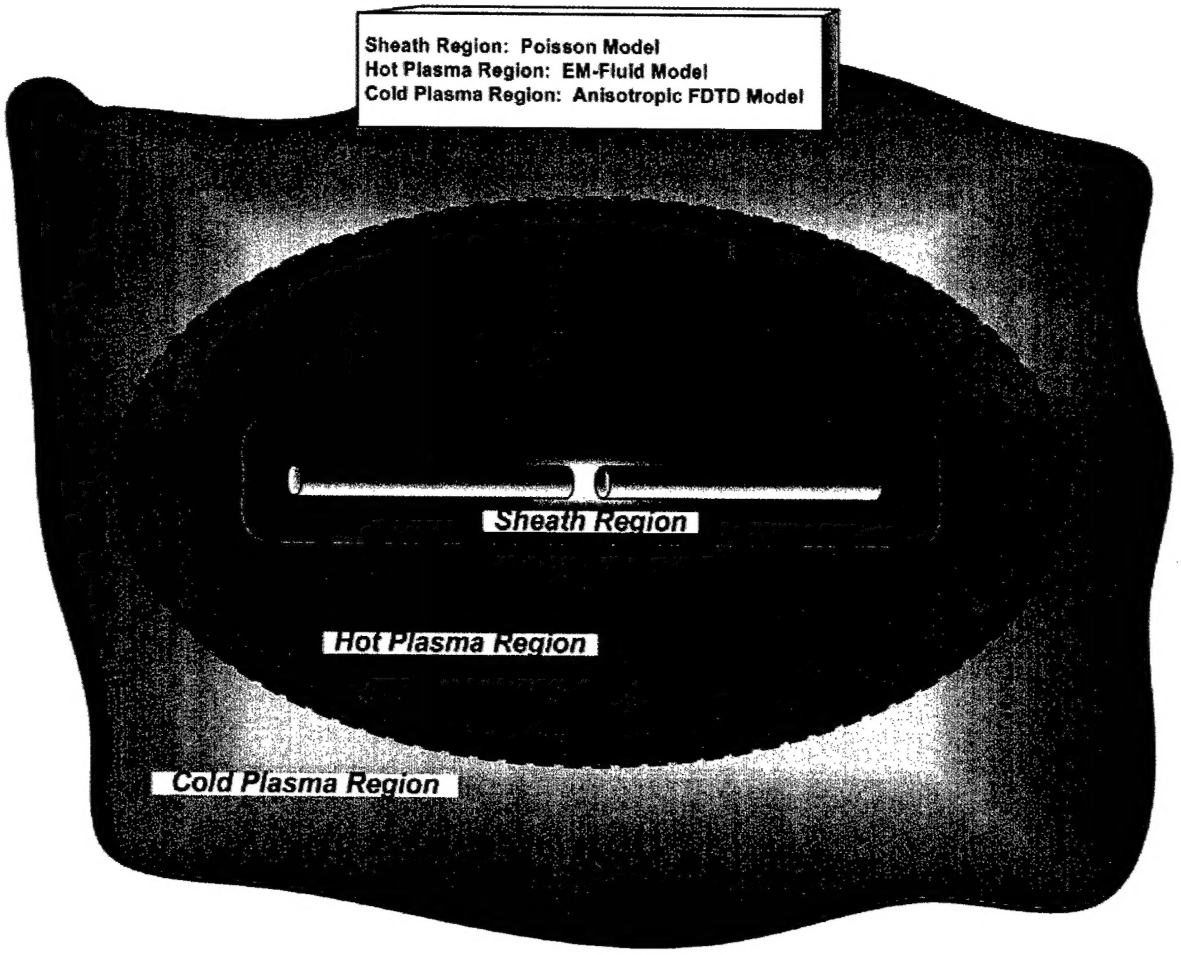

Figure 1. Regions of Simulation Space

A.1 Full EM Fluid Code

The Full Electromagnetic Fluid Code is applied to region 2 of Figure 1 and includes Maxwell's equations for modeling the electromagnetic and electrostatic portion of the code, and a fluid model for determining the first three moments of the Boltzmann equation including conservation of number density, momentum, and energy for one species of ion and electrons. The equations are listed as follows:

$$\frac{\partial \rho}{\partial t} + \nabla \cdot (\rho \mathrm{u}) = S^{\rho}$$

$$\frac{\partial \rho \mathrm{u}}{\partial t} + \nabla \cdot (\rho \mathrm{uu}) = -\nabla \cdot \Pi + q\eta(\mathrm{E} + \mathrm{u} \times B) + \mathrm{u}S^{\rho} + \mathrm{S}^{\mathrm{m}}$$

$$\frac{\partial}{\partial t}\left(\frac{1}{2}\rho u^2 + \frac{1}{\gamma - 1}p\right) + \nabla \cdot \left(\frac{1}{2}\rho u^2 \mathrm{u} + \frac{1}{\gamma - 1}p\mathrm{u} + \mathrm{u} \cdot \Pi + L\right) = q\eta \mathrm{u} \cdot \mathrm{E} + \frac{1}{2}u^2 S^{\rho} + \mathrm{u} \cdot \mathrm{S}^{\mathrm{m}} + S^{U}$$

$$\nabla \times \mathrm{E} = -\frac{\partial B}{\partial t}$$

$$\nabla \times H = J + \frac{\partial \varepsilon_0 \mathrm{E}}{\partial t} \qquad \mathrm{J} = \eta_e q_e \mathrm{u}_e + \eta_i q_i \mathrm{u}_i$$

S^{α} = sources
ρ = mass density
p = pressure
η = number Density
u = Bulk Velocity of Particles
E = electric Field
$\mathrm{B} = B_0 + \tilde{\mathrm{B}}$ = Static Magnetic Field + Wave Magnetic Field
m = mass
Π = pressure tensor
L = heat flux
J = current density

A number of simplifications can be made depending upon where in the magnetosphere the antenna will be operating. Since it is envisioned that the antenna will be operating on a spacecraft near the magnetic equatorial plane at L=2 or 3, the electron and ion number densities will be relatively low compared to low Earth orbit. In this region the densities are on the order of 10^9 /m^3, and the plasma is fully ionized and collisions are negligible. This means that all terms involving collisions are zero, and that shearing and viscous forces are non-existent, so that the pressure tensor is isotropic, given by the ideal gas law, and there is no diffusion. Using these simplifications, the fluid equations can be reduced to the following equations which are written in conservative form:

$$\frac{\partial U}{\partial t}+\frac{\partial F(U)}{\partial x}+\frac{\partial G(U)}{\partial y}+\frac{\partial H(U)}{\partial z}=S$$

$$U=\begin{bmatrix}\eta\\ \eta u_x\\ \eta u_y\\ \eta u_z\\ E\end{bmatrix},\ \mathrm{F}=\begin{bmatrix}\eta u_x\\ \eta u_x^{\,2}+p\\ \eta u_x u_y\\ \eta u_x u_z\\ u_x(E+p)\end{bmatrix},\ \mathrm{G}=\begin{bmatrix}\eta u_y\\ \eta u_y u_x\\ \eta u_y^{\,2}+p\\ \eta u_y u_z\\ u_y(E+p)\end{bmatrix},\ \mathrm{H}=\begin{bmatrix}\eta u_z\\ \eta u_z u_x\\ \eta u_z u_y\\ \eta u_z^{\,2}+p\\ u_z(E+p)\end{bmatrix},\ \mathrm{S}=\begin{bmatrix}0\\ \frac{q\eta}{m}(\mathrm{E}_x+u_y(B_{0z}+\widetilde{B}_z)-u_z(B_{0y}+\widetilde{B}_y))\\ \frac{q\eta}{m}(\mathrm{E}_y+u_z(B_{0x}+\widetilde{B}_x)-u_x(B_{0z}+\widetilde{B}_z))\\ \frac{q\eta}{m}(\mathrm{E}_z+u_x(B_{0y}+\widetilde{B}_y)-u_y(B_{0x}+\widetilde{B}_x))\\ q\eta(\mathrm{E}_x u_x+\mathrm{E}_y u_y+\mathrm{E}_z u_z)\end{bmatrix}$$

$$E=\frac{1}{2}m\eta u^2+\frac{1}{\gamma-1}p$$

$$p=(\gamma-1)\left\{E-\frac{1}{2}m\eta \mathrm{u}^2\right\}=\text{pressure}$$

γ = degrees of freedom

Maxwell's equations are used for the calculation of the both the radiation pattern of the antenna and quasi-electrostatic effects near the sheath. Used in conjunction with the fluid equations, the number densities and velocities are used to update the corresponding conduction current term in the curl equation for the magnetic field.

Maxwell's equations are solved using a well-established FDTD (Finite Difference Time Domain) method. The fluid portion of the code is more complicated since it incorporates nonlinearities which may give rise to a number of fluid phenomena such as shocks that would render many finite difference schemes unstable. The fluid portion of the code is solved using the method outlined in [*Kurganov and Tadmor, 2000*]. This method involves incorporating a small amount of artificial viscosity into the code to smooth out any numerical artifacts that come about due to the nonlinear terms present in the fluxes. The artificial viscosity is proportional to the maximum characteristic speeds in the plasma which can be found by taking a Jacobian of the flux matrices. This technique has been proven very accurate for systems of conservation laws [*Kurganov and Tadmor, 2000*].

As in all finite difference methods, a mesh is used to discretize continuous space, and all the derivatives are solved using samples of this space. The configuration for this model is shown in Figure 2, representing a dipole in three-dimensional space. All fluid variables are located at the cell centers. Electric fields are located at the cell edges, and magnetic fields as well as fluxes are located at the cell faces.

As a result of the FDTD method used to solve for the radiated fields, E + H are staggered in both time and space. The fluid variables must therefore take this into account.

Since the fluid variables are solved using a forward time centered space (FTCS) representation, the fluid variables must be co-located in time with either E or H. We chose the fluid variables to be co-located temporally with the magnetic field.

Because of this, both the old and new time steps for the electric field must be stored in different arrays. The temporal arrangement for the different variables is shown in Figure 3.

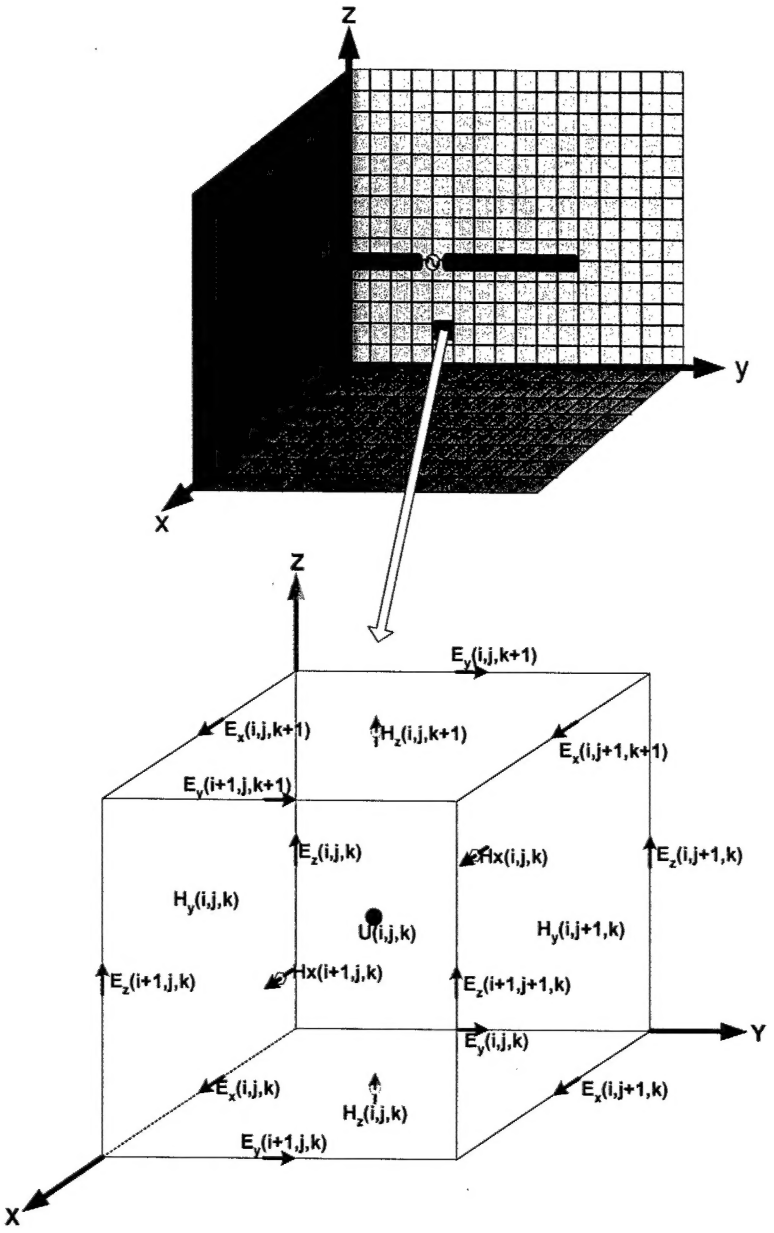

Figure 2. Mesh and Cell Configuration

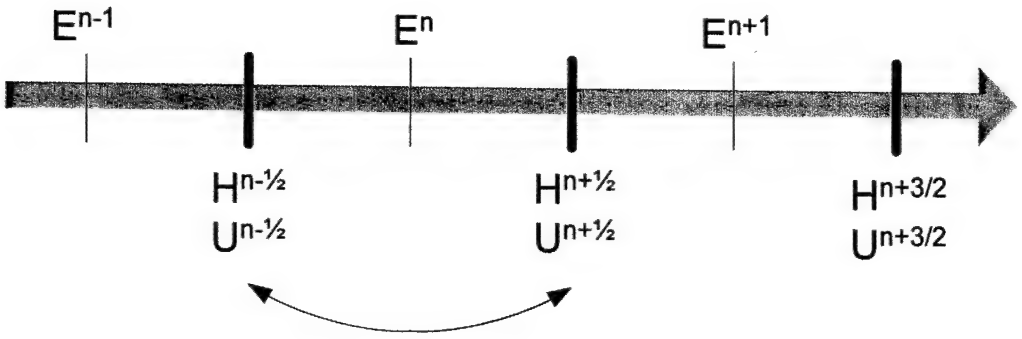

Since the fluid variables U are solved with a forward time scheme, U must be updated using values located at the previous time step and not half way in between like FDTD. Therefore to solve for $U^{n+½}$, the variables $U^{n-½}$,$H^{n-½}$, and the average of E^{n} and E^{n-1} must be used. Hence the need to store the old values of Electric Field.

Figure 3. Orientation of Variables along time axis

In an FDTD method, the antenna is excited by applying a potential difference between the two conductors of a dipole as shown in Figure 4. Once the antenna is excited (via electric field enforcement) the fluid and magnetic field values are determined using the newly acquired electric field value, and finally the updated electric field is determined using the fluid and magnetic field variables that were just calculated. We use the Fluid code to find the antenna current distribution in the following way. The sinusoidally varying potential is applied in the gap between the conductors. The voltage and current waveforms propagate along the antenna setting up the correct distributions for a radiating element. The electromagnetic and induction fields are mapped from the vicinity of the antenna out to the sheath boundary assuming a 1/r variation. The effects of the sheath are introduced through a boundary condition on the

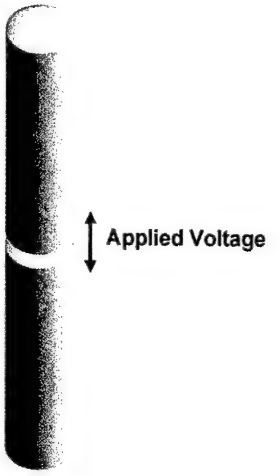

1.) Antenna Excitation
2.) Solve for Fluid Variables (Number density, Momentum, and Energy)
4.) $\nabla \times E = -\frac{\partial B}{\partial t}$ (Solve for H)
5.) $\nabla \times H = J + \frac{\partial D}{\partial t}$ (Solve for E)
6.) Repeat steps 1 - 5 until convergence

Figure 4. Antenna Excitation

radial component of the quasi-static electric field. at the sheath edge.

A.2 Boundary Conditions

The correct boundary conditions are perhaps the most important part of any simulation. Boundary conditions in this model are made for the truncation of both the FDTD and fluid lattice as well as the boundary conditions for fluxes onto the antenna surface. Since it is important that both electrostatic and electromagnetic waves do not reflect back from the boundary, absorbing boundary conditions have been developed for both the fluid and Maxwell's equations. Absorbing boundary conditions for the solution of Maxwell's equations are well known. Perhaps the most notable and promising is the PML (Perfectly Matched Layer) formulation introduced in [*Berenger, 1994*]. This requires a thin layer of cells around the FDTD space which simulate a highly absorptive media. A better implementation of this method is discussed in [*Roden and Gedney, 2000*] which allows for the absorption of evanescent modes and is completely independent of the host medium. This is the method of choice for the EM-fluid model presented here. Since the method utilizes a convolution operator, the equations must be approximately linear for the method to work. It has been shown that this methods has an effective absorption rate of up to 50-100 dB of the incident wave.

The PML method works well for Maxwell's equations, however the nonlinear fluid equations are much more of a challenge. Some assumptions must be made. Equivalent methods for fluid dynamics are not yet available for non-linear equations [*Hesthaven. 1997*]. However, a number of aspects particular to the problem at hand allows for the use of this convolutional PML derivation. Outside of the sheath region, the bulk velocity of the plasma is essentially zero. Meaning that there is no mean fluid flow. All other quantities are small relative to the ambient values. This means that the convective terms in the fluid equations are essentially zero, allowing for the linearization of the fluid equations. Boundary conditions for a zero mean flow essentially reduce to those involving wave equations such as Maxwell's, thus we can apply the same PML scheme to the fluid equations. Absorbing boundary conditions must be implemented for each model region (refer to Figure 1) in order to prevent contamination from spreading into each successive calculation.

Boundary conditions for the conductor must also be taken into account. In many papers, it is assumed that the particles hit the walls of a conductor with the thermal velocity. The unidirectional continuity flux of particles at the wall is thus given by:

$$\Gamma = \frac{1}{4}\eta v_{th}$$

[*Lymberopoulos, Economou. 1995*]. Some papers also include a secondary emission coefficient [*Meezan, Capelli. 2001*]. In the magnetosphere at L=2 in the magnetic equatorial plane, the plasma temperature is only about 1/5eV. Therefore any potential in the kV range will accelerate electrons well above the thermal velocities and this must be taken into account. Therefore, boundary conditions similar to those found in [*Lymberopoulos and Economou, 1995*] are used in this model including secondary electron emission with the exception that the velocity of the particles is actually the sum of the thermal velocities into the wall and the bulk fluid velocity at the wall as shown in Figure 5. Boundary conditions involving thermal velocities are implemented for the continuity and energy equations. It is assumed the there is no gradient in any of the conserved quantities at the wall of the conductor.

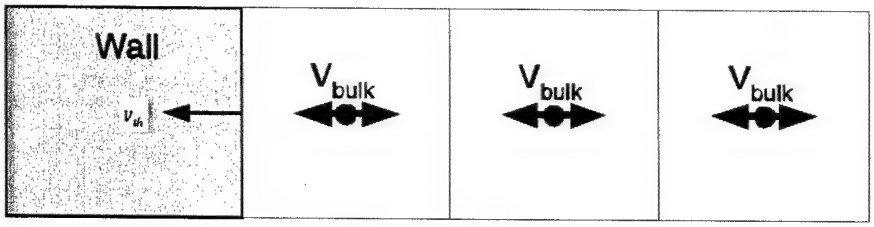

$$v_{wall} = v_{th} + v_{bulk}$$

Figure 5. Fluid Boundary Condition

A.3 Antenna Pattern

Once the number densities reach a steady state distribution, the antenna currents and the currents within the sheath region are used to determine the antenna pattern using a far-field transformation (Fig. 6). The far field transformation involves the use of the radiated electromagnetic fields E and H, Green's Theorem and the Surface Equivalence Theorem. The radiated fields within the problem space can be weighted by the free space Green's function and integrated around a closed surface to provide the far-field pattern of the antenna.

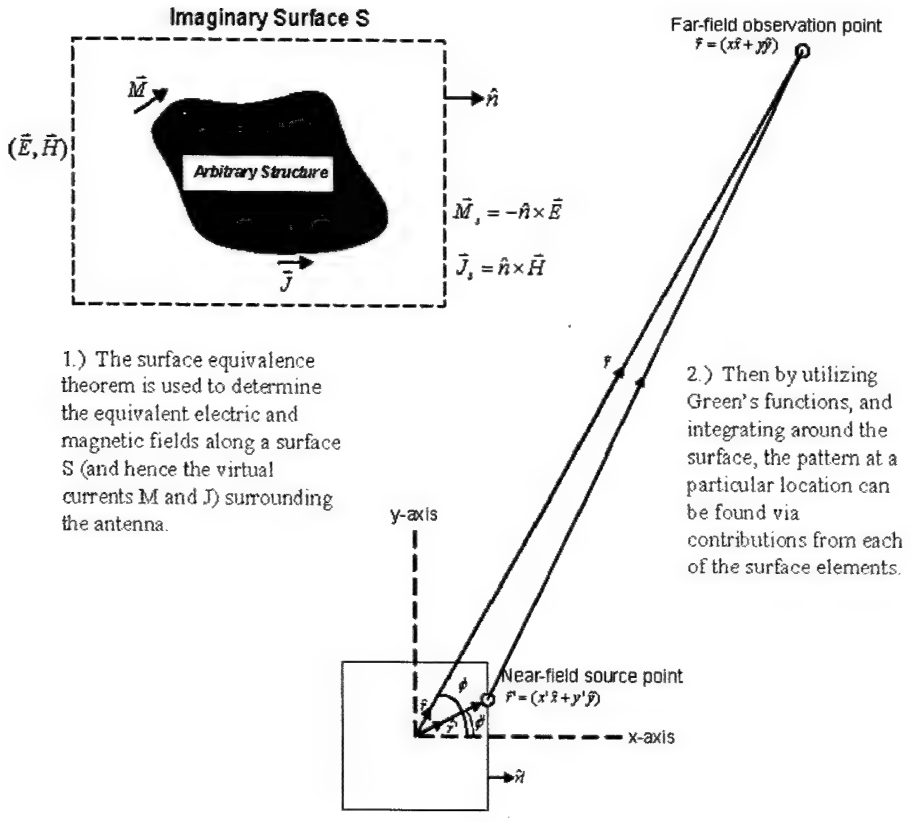

Figure 6. Near-field to Far-field Transformation

A.4 Requirements of the full EM-fluid formulation

There are a number of requirements, which must be met in order to properly use the full EM-fluid model. In order for the boundary conditions to work effectively, the truncation of the space must occur in a region where the assumptions in which the boundary equations were formulated are satisfied. For instance, one must be in the far-field for the PML condition to work for Maxwell's equations, and for the fluid equations, the space must be far enough beyond the sheath region for the cold-plasma approximation to be satisfied, i.e. any non-linear equations must be well approximated by linear versions. Since both Maxwell's and the fluid equations are solved simultaneously, the far-field condition for Maxwell's equation (being the greater of the two) takes precedence.

An option exists to reduce the number of cells necessary for the simulations, known as the AMR (Adaptive Mesh Refinement) technique. It involves applying resolution only where it is necessary, such as around the radiating structure, where electrostatic effects such as sheath development must be considered. This method is useful in any model in which multiple wavelengths exist at once, such as the electrostatic sheath model, or in an anisotropic FDTD model where the refractive index changes with both frequency and angle with respect to the magnetic field. A diagram of this concept is displayed in Figure 7 where the dipole antenna is shown in the middle of the space. This method has been developed for variables that are located at cell centers or cell faces such as the fluxes and fluid variables in the fluid equations. However, in the case of FDTD for Maxwell's equations, the electric fields are located at the cell edges, to allow for an accurate curl representation. The current AMR method is not applicable to this case, however we estimate that appropriate modifications to the AMR method for use in our simulations could be completed in 3-6 months.

Concept of Adaptive Mesh Refinement (AMR) for Antenna Problem
Largest Cell Size ~ 100m
Smallest Cell Size ~ .01m
This means that the problem requires about 14 levels of refinement if each level of refinement is considered to be a reduction by 2 in cell size

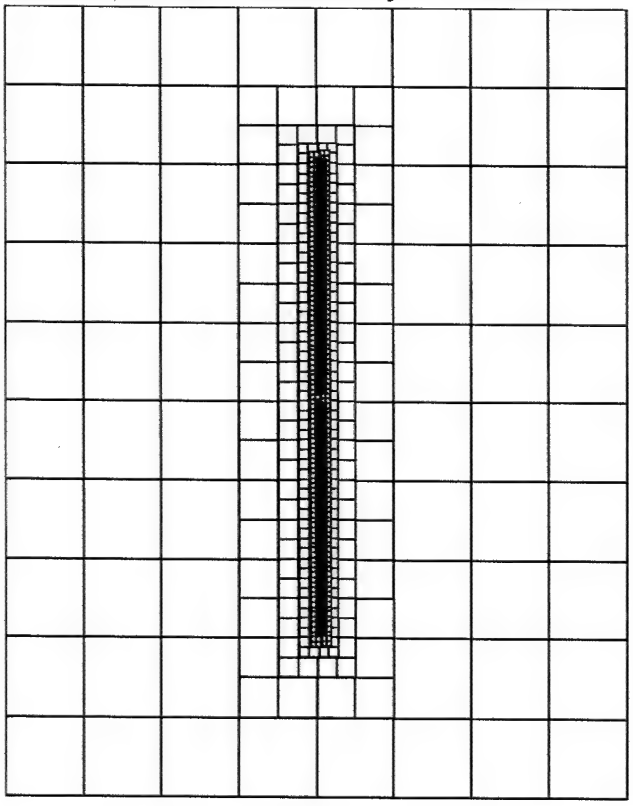

Figure 7. AMR (Adaptive Mesh Refinement)

A.5 Poisson Model for the Sheath

. At potentials in the kV range, the sheath may be on the order of a few meters in radius. Since the driving frequency of the antenna will generally be much less than both the electron and ion plasma frequencies, the sheath should reach a quasi-steady state at each point in the sinusoidal cycle. Therefore at each point in the sinusoidal variation, the sheath should expand and collapse with the potential of the driving elements. The characteristics of the sheath dimensions and the dynamics of the charged particles within the sheath can then be determined through a simulation involving a Poisson model.

The Poisson model involves solving the fluid equations with electric field source terms determined through the use of Poisson's equation.

$$\nabla^2 \Phi = -\frac{\rho}{\varepsilon_0}$$

Poisson's equation is solved using a fast-sine transform, which falls under the category of rapid elliptic solvers. This technique proved to be the most efficient method for solving elliptic equations of this sort. To place conducting objects at specified potentials, it is necessary to incorporate a capacity matrix method, which allows sources internal to the system to be placed inside the space and provide a correct solution of Poisson's equation [*Hockney and Eastwood,* 1981].

In using a Poisson type technique it is assumed that the potential is constant along each dipole element. This is equivalent to assuming a triangular current distribution along the antenna, which is the distribution expected for antennas whose length is much shorter than a wavelength. In the Poisson approach, the potentials are applied on each of the conductors independently as shown in Figure 8, however the magnitude of the applied potentials is assumed to vary sinusoidally.

Two constant potentials of +V and -V are applied across the entire conductor in this electrostatic case (The voltage waveform is a constant across the length of the conductor)

Figure 8. Poisson Model

The timestep constraint for Poisson type models is well documented as being the minimum of either the inverse of the plasma frequency, that which is related to the maximum characteristic speed in the plasma based on thermal effects and bulk velocities, or the dielectric relaxation time if the plasma is collisional which is often the most restrictive of the timesteps. Since the plasma in the current formulation is collisionless, the last constraint does not apply. For the operating conditions of this model, the maximum characteristic speeds in the plasma are generally the determining factor. In our case, the timestep corresponding to the thermal velocities are more restrictive than those having to do with plasma oscillations. And for a 0.2 eV plasma, and applied potentials on the antenna of 1000V or more, the bulk velocities almost always exceed the thermal velocities in a collisionless regime.

Trying to resolve a steady state solution on small grids with very low frequency waves poses a challenging problem at the present time, but the complexity can be reduced to manageable levels using the AMR technique. An alternative approach exists which involves the solution of Poisson's equation for a slowly varying applied potential over subsections of the large antenna whose lengths are much larger than the sheath radius. By slowly varying we mean that the frequency of the applied potential is much smaller than either the electron or ion plasma frequency, which will generally be the case for the proposed VLF radiating system. In this way the sheath characteristics as a function of applied potential could be calculated along the entire antenna. Using these sheath characteristics developed in the Poisson model, it would then be possible to implement a dynamic sheath into an FDTD approach. Essentially, this involves merging the electrostatic and electromagnetic models as outlined in Figure 1.

A.6 Anisotropic Cold Plasma FDTD Model

In region 3 of Figure 1, the simulation model involves the solution of Maxwell's equations in a cold plasma and the propagation of ELF/VLF waves in this inhomogeneous, anisotropic medium. Once the currents in regions 1 and 2 of Figure 1 are specified, the cold plasma model can then be used to determine the radiation fields produced by these currents. This is an alternative method to that shown in Figure 6. The model involved utilizes the method outlined in [*Lee and Kalluri,* 1999]. This includes the solution of the following equations:

$$\nabla \times E = -\mu_0 \frac{\partial H}{\partial t}$$

$$\nabla \times H = \varepsilon_0 \frac{\partial E}{\partial t} + J$$

$$\frac{\partial J}{\partial t} + \nu J = \varepsilon_0 \omega_p{}^2(r,t)E + \omega_b(r,t) \times J$$

Here, ε_0 is the free space permittivity, μ_0 is the free space permeability, ν is the collision frequency, ω_p is the plasma frequency, and ω_b is the electron gyrofrequency. Warm plasma effects can be introduced through a pressure term when necessary [*Young and Brueckner,* 1994]. These equations can be used to accurately model wave propagation outside of the sheath and hot plasma regions. To demonstrate the validity of the model, we present a series of plots showing a simple cold plasma regime with operating points specified on the w-k diagram shown in figure 8.

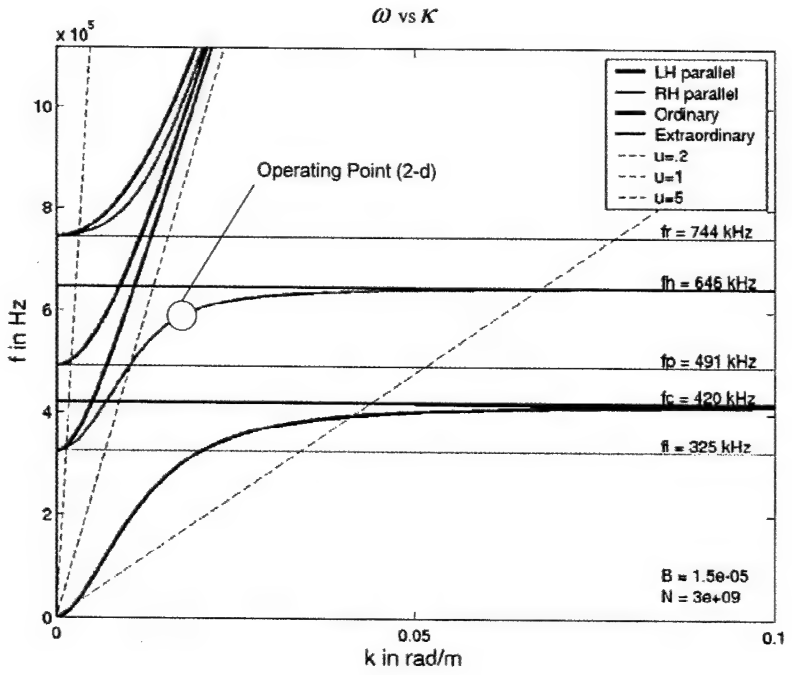

Figure 9. ω-k diagram

The model however, was thoroughly tested in 1-d for points on the ordinary and parallel branches as well. The model accurately depicted cutoff regions and displayed appropriate wave numbers for the test cases.

In the following section, the validity of the multidimensional anisotropic model in a cold plasma is demonstrated. Both free space propagation and that within a plasma are presented. A 2-dimensional coordinate system is set up to allow for calculation of both the free space and extraordinary modes on the w-k diagram. In the following 2-d models, the antenna is a ½λ dipole with Hz, Ex, and Ey as the field configuration and a static magnetic field directed in the z-direction. The antenna elements are in the x-y plane with the antenna oriented along the y-direction and infinite in extent in the z-direction as shown in Figure 10. The antennas are excited via a potential difference across the gap between the elements in the y-direction (Ey excitation).

A plot of the Fourier transform of the spatial frequency is also displayed. This will provide a comparison for the cold plasma case. The following figures will show the same dipole configuration for an antenna operating in the plasma at the location specified by the operating point in Figure 9. The 2-d simulation plots shown with the exception of the free space diagram will be those representing the extraordinary branch of the w-k diagram.

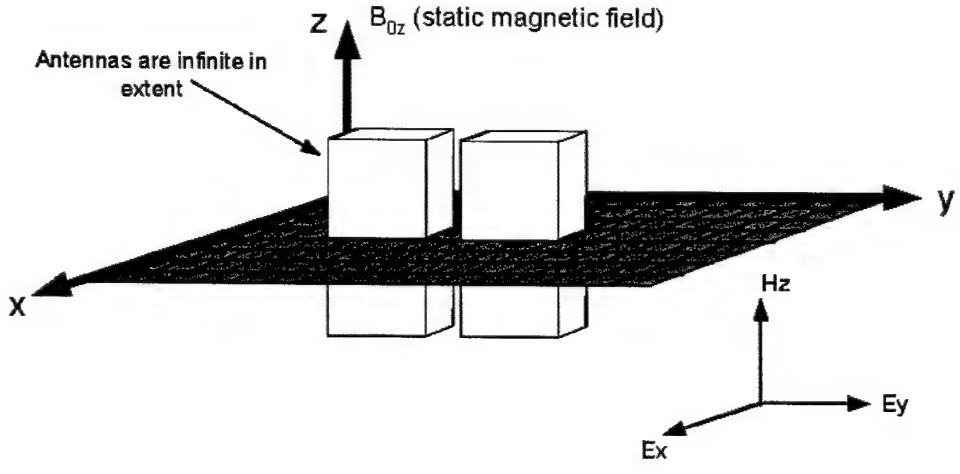

Figure 10. 2-d antenna simulation

Figure 11 shows the plot of the free space Ey field after 17 cycles at 491kHz. The spatial Fourier transform at this time step is plotted in Figure 12 and a zoom in of the FFT is displayed

in Figure 13. At an operating frequency of 491kHz in free space, the wavelength should be 610 m and the spatial frequency should be about .0016 1/m.

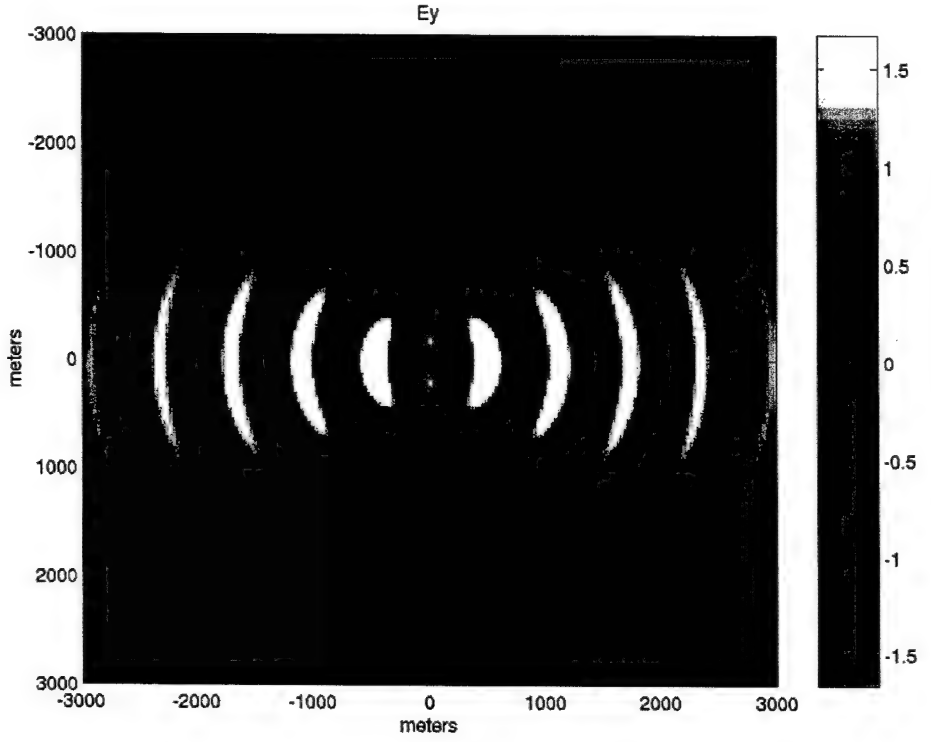

Figure 11. Ey field in free space

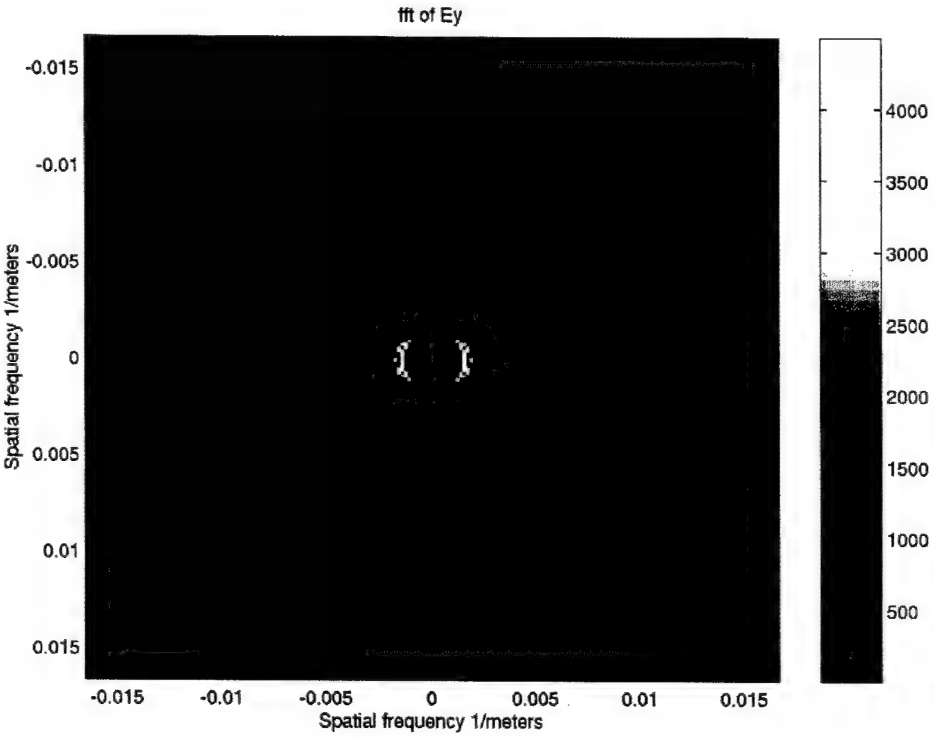

Figure 12. FFT of Ey field

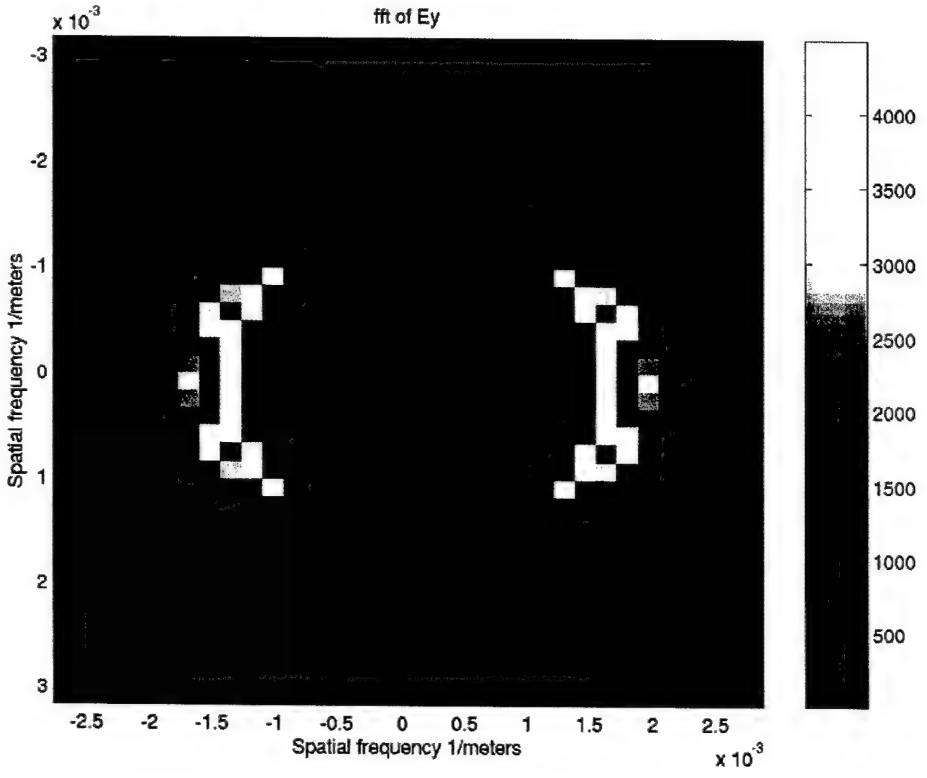

Figure 13. Enlargement of Ey field FFT

It can bee seen from the plot that the spatial frequency is indeed 1.6e-3 1/m as one would expect. Figure 14 shows the propagation of the Ey field for the free space case over a period of 1 cycle of the operating frequency.

To test the validity of the anisotropic model, the extraordinary branch at a frequency of 625 kHz was modeled. At this frequency, the refractive index is equal to 2. Therefore the wavelength should be ½ of the free space value. For the anisotropic case, this spatial frequency should be .0042 1/meters. The same set of plots is made for the Ey field in the cold plasma. Figure 15 shows the Ey field. Figure 16 and 17 show the FFT and enlargement of the FFT for this field after 17 cycles. Once again good agreement is obtained. Figure 18 is another sequence of the Ey field over 1 period for the anisotropic case.

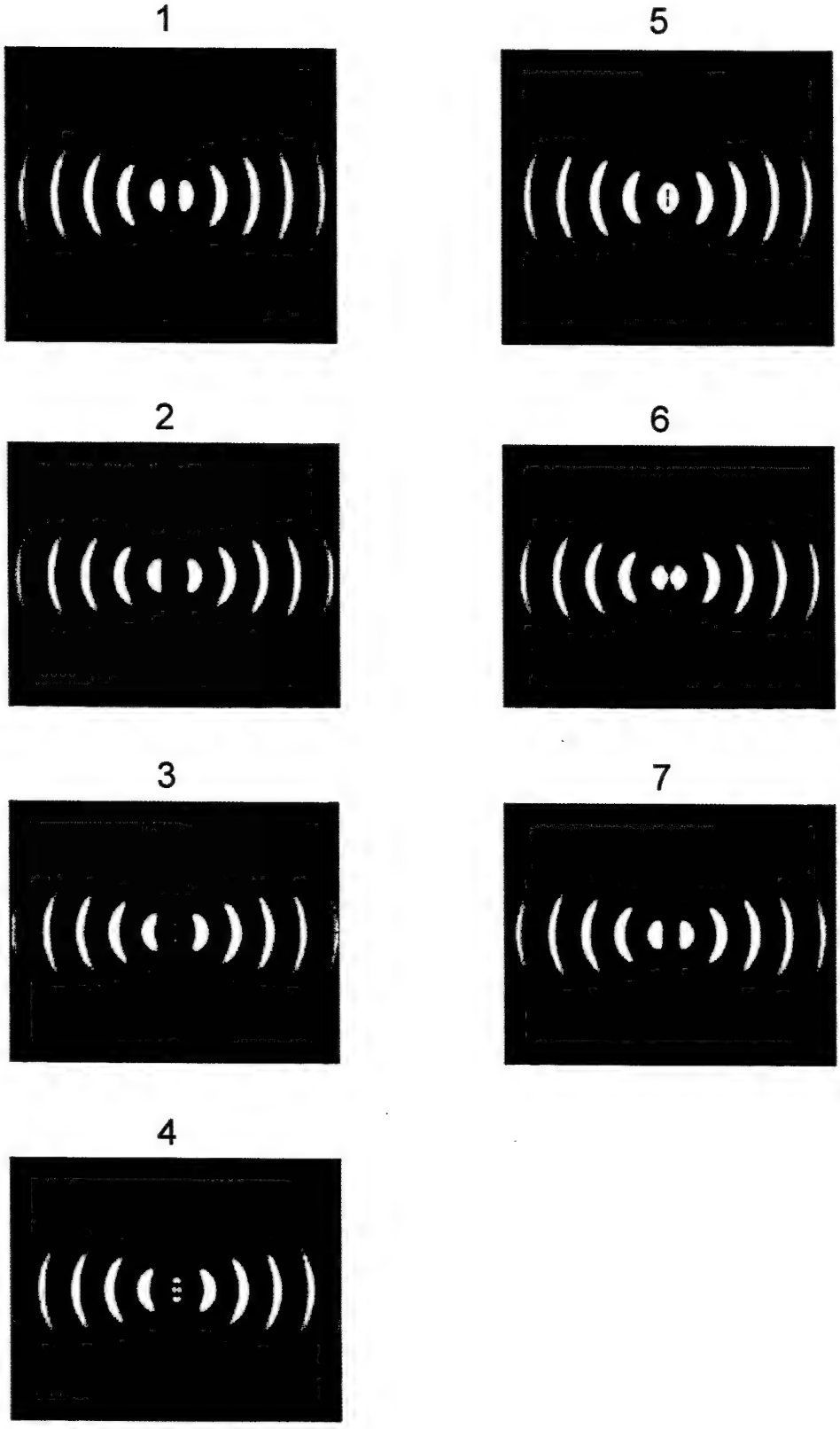

Figure 14. Ey Sequence

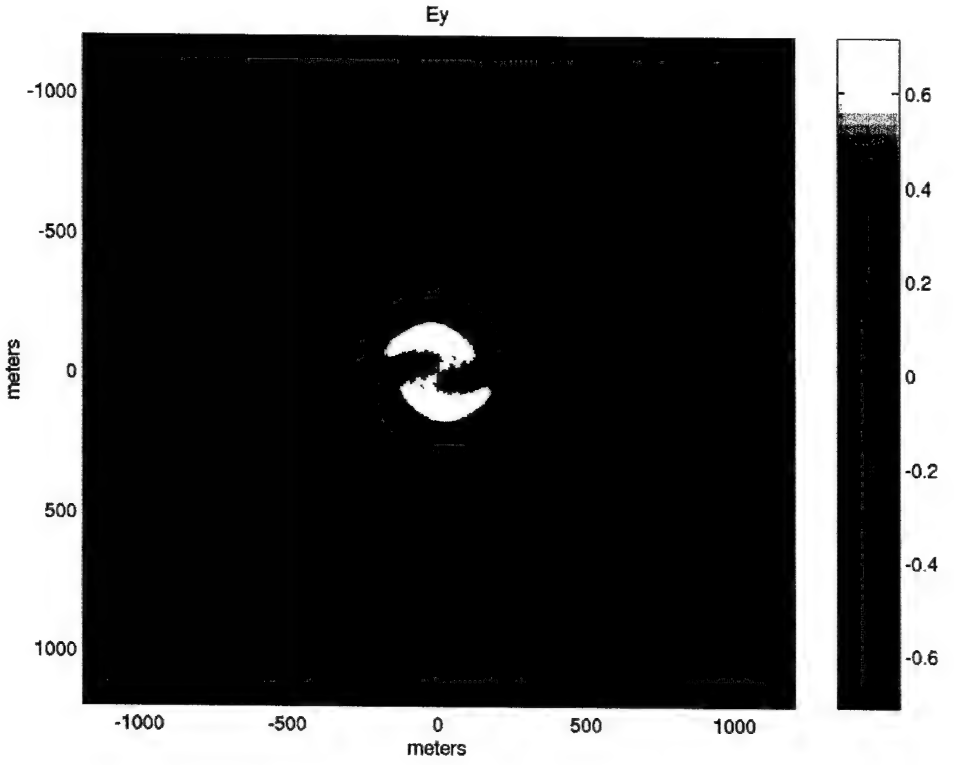

Figure 15. Ey field in Cold Plasma

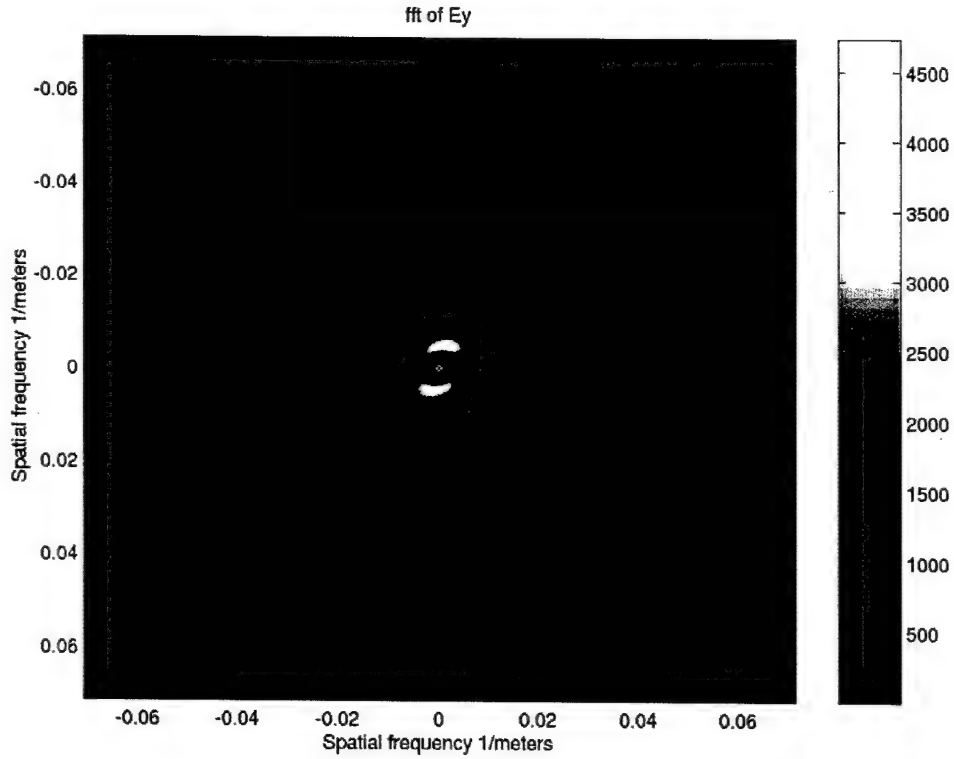

Figure 16. FFT of Ey field in Cold Plasma

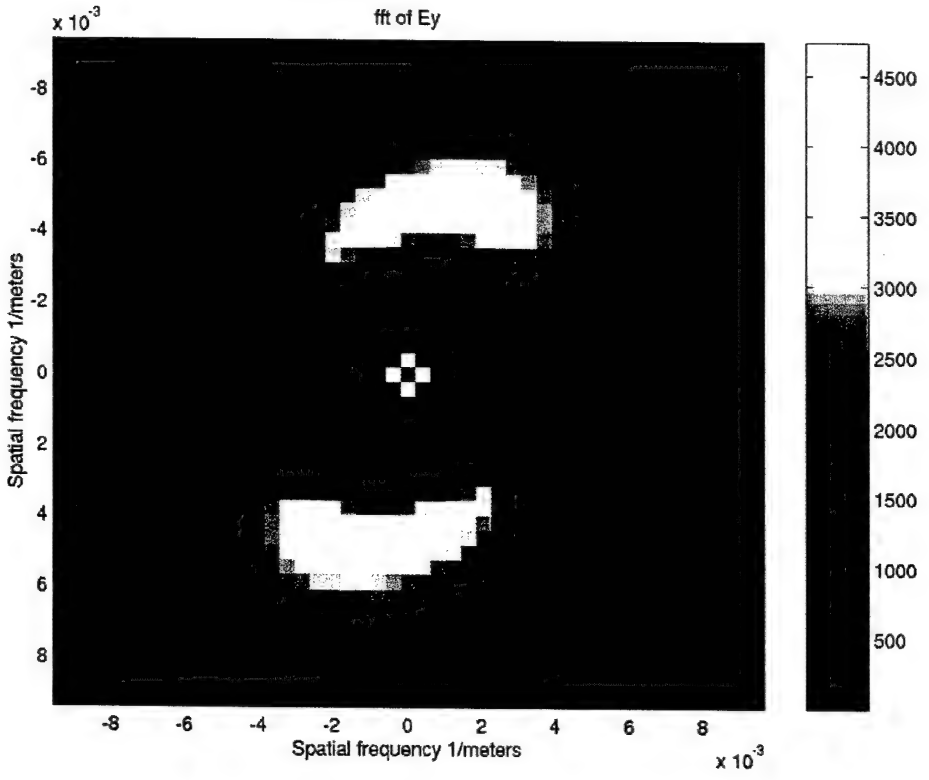

Figure 17. Enlargement of Ey field FFT in Cold Plasma

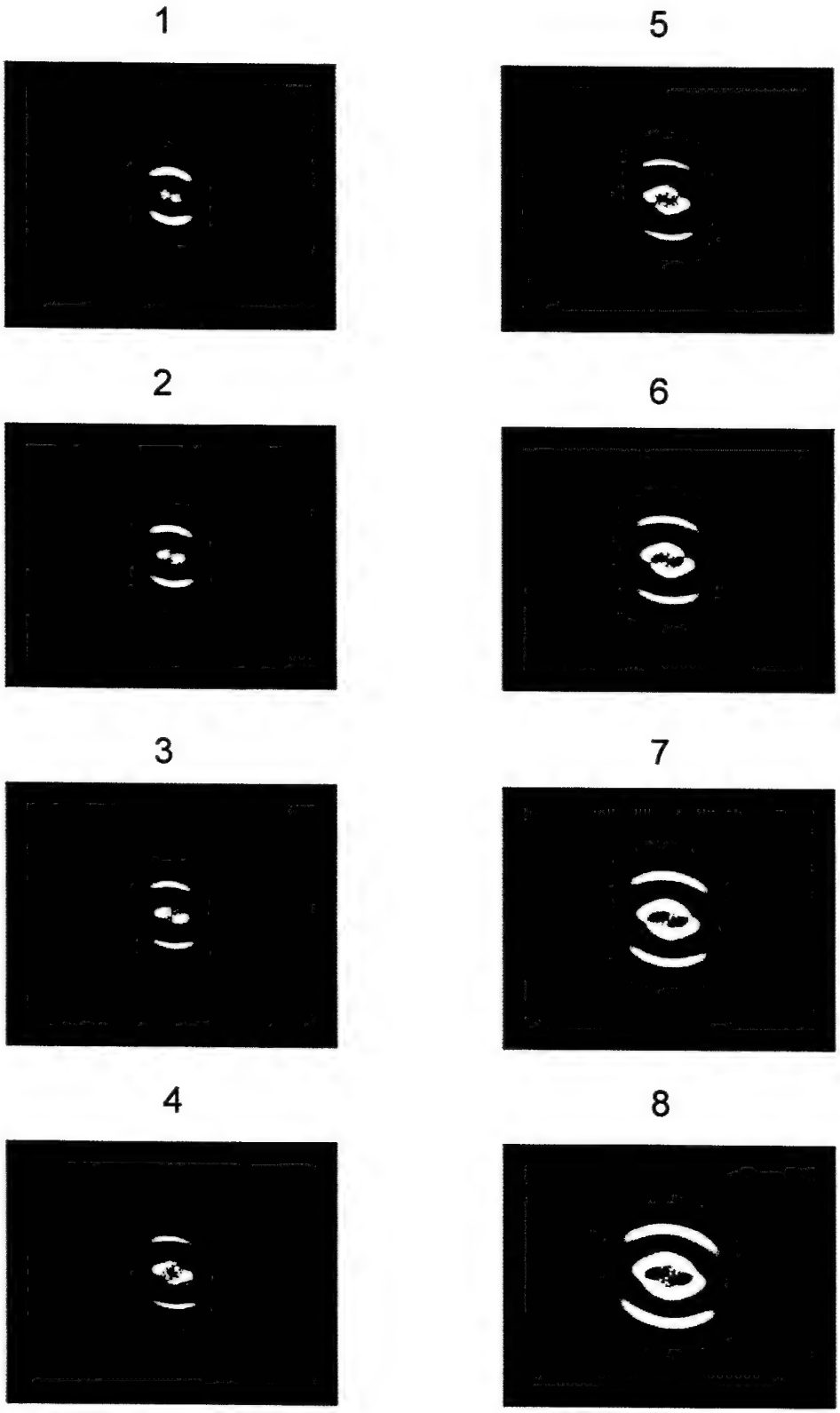

Figure 18. Ey Sequence in Cold Plasma

The final case is a three dimensional run made at the location defined as the operating point on Figure 19 which corresponds to 15kHz. In this case all components of E, H, and J are used in the simulation. The model is being run at a frequency corresponding to the whistler mode. The same configuration of antenna and static magnetic field as in the 2-d case are used. The static magnetic field is oriented in the z-direction and the antenna along the y-direction in the x-y plane. The only difference is that the z-dependence of the variables is added. It can be seen, that as expected, the fields are directed toward the static magnetic field, which is in the z direction. Sequences of slides for the three slices through the antenna are shown on the following pages for the Ey component which is the field of excitation on the antenna. Evanescent modes are seen in the x-y plane, and propagation is seen within a very small cone centered along the z-direction as expected. Since in FDTD it is necessary to resolve the smallest wavelength in the system, collisions were added to control the effects at the resonance cone where $\lambda \rightarrow 0$.

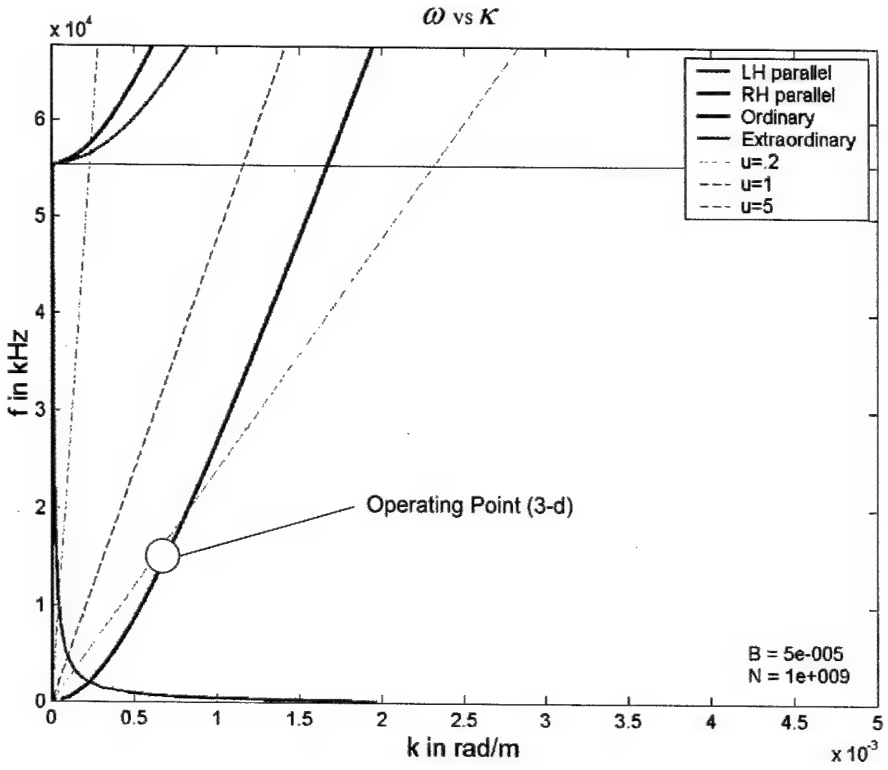

Figure 19. ω-k diagram

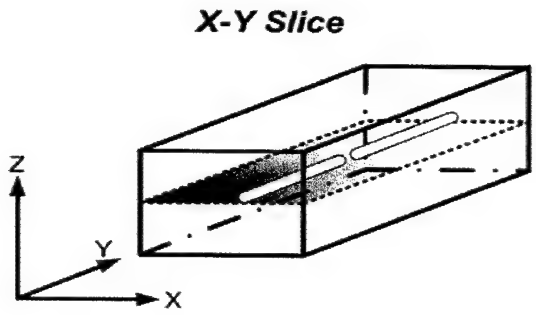

Figure 20. XY plane through antenna

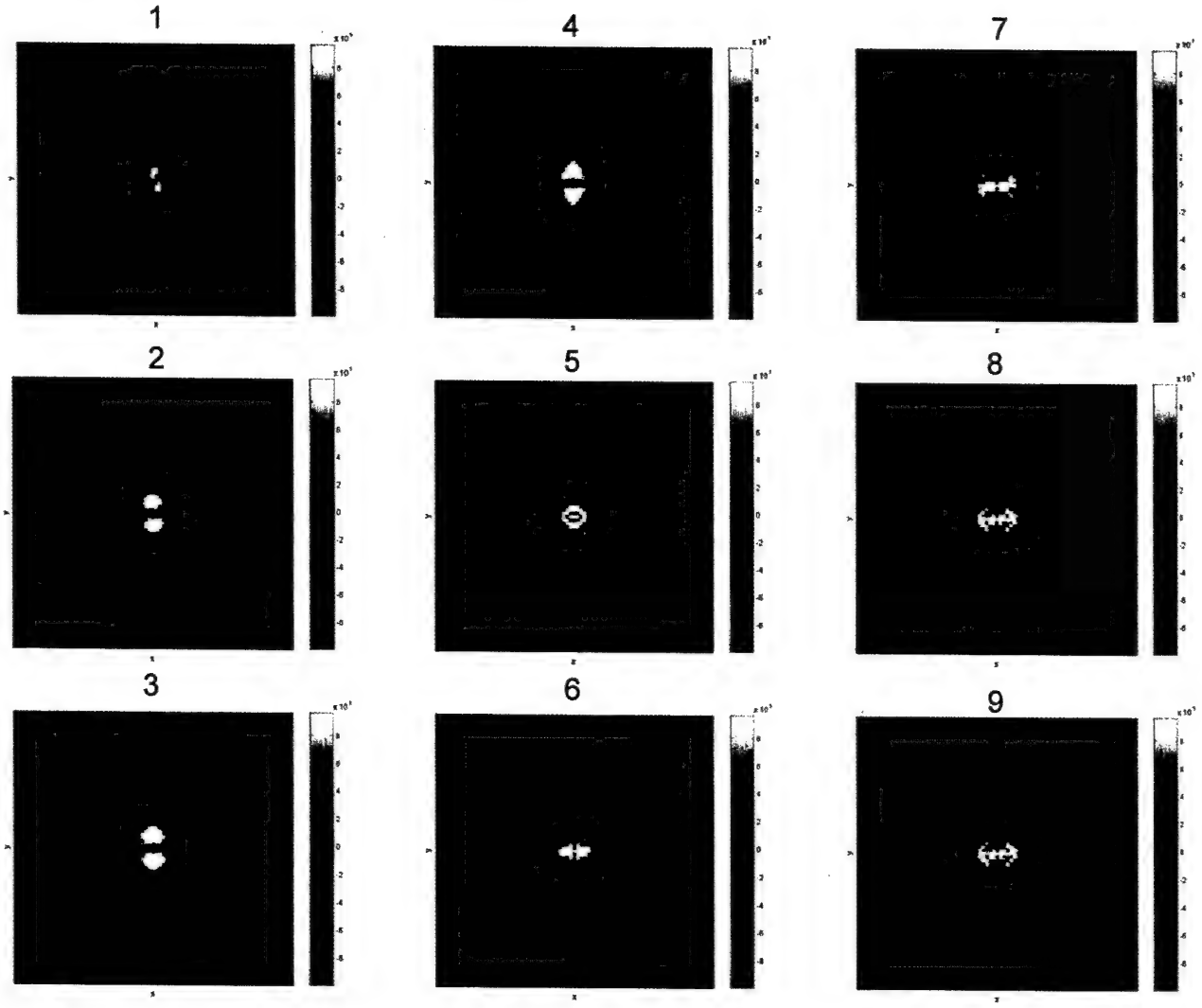

Figure 21. Ey field in X-Y Plane (Evanescent)

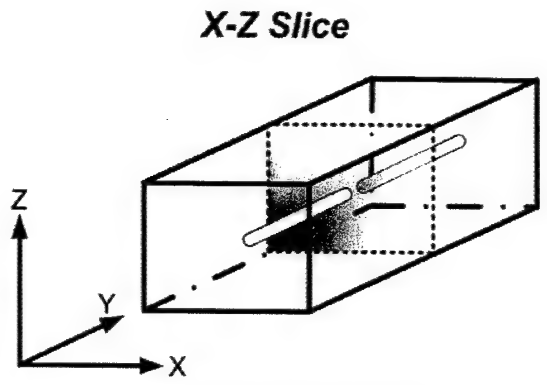

XZ plane through antenna

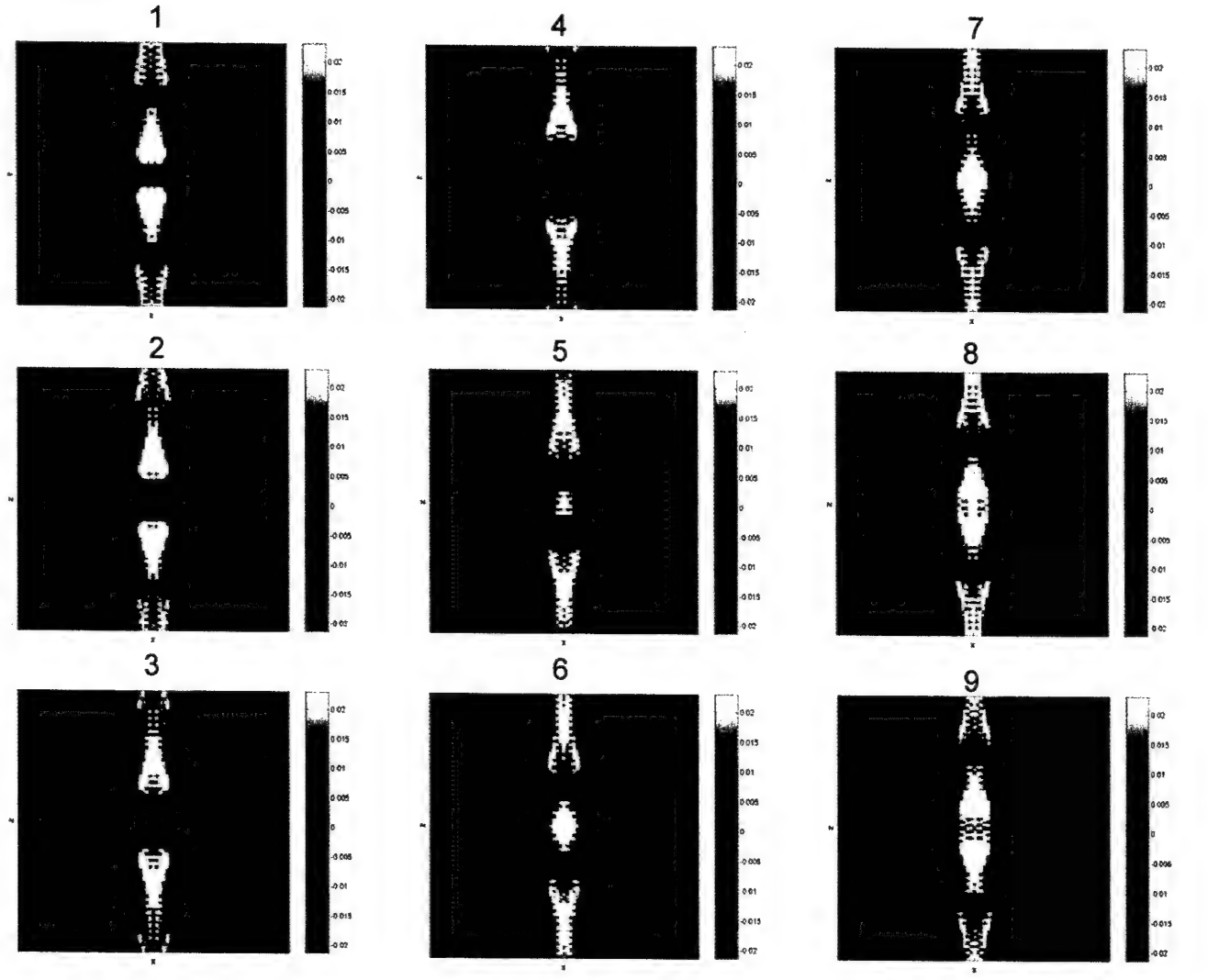

Figure 22. Ey field in X-Z Plane. Propagation along Z.

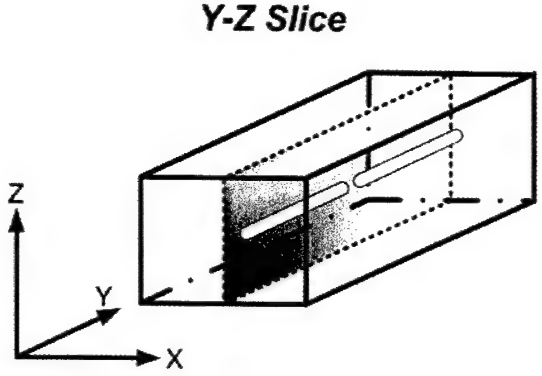

YZ plane through antenna

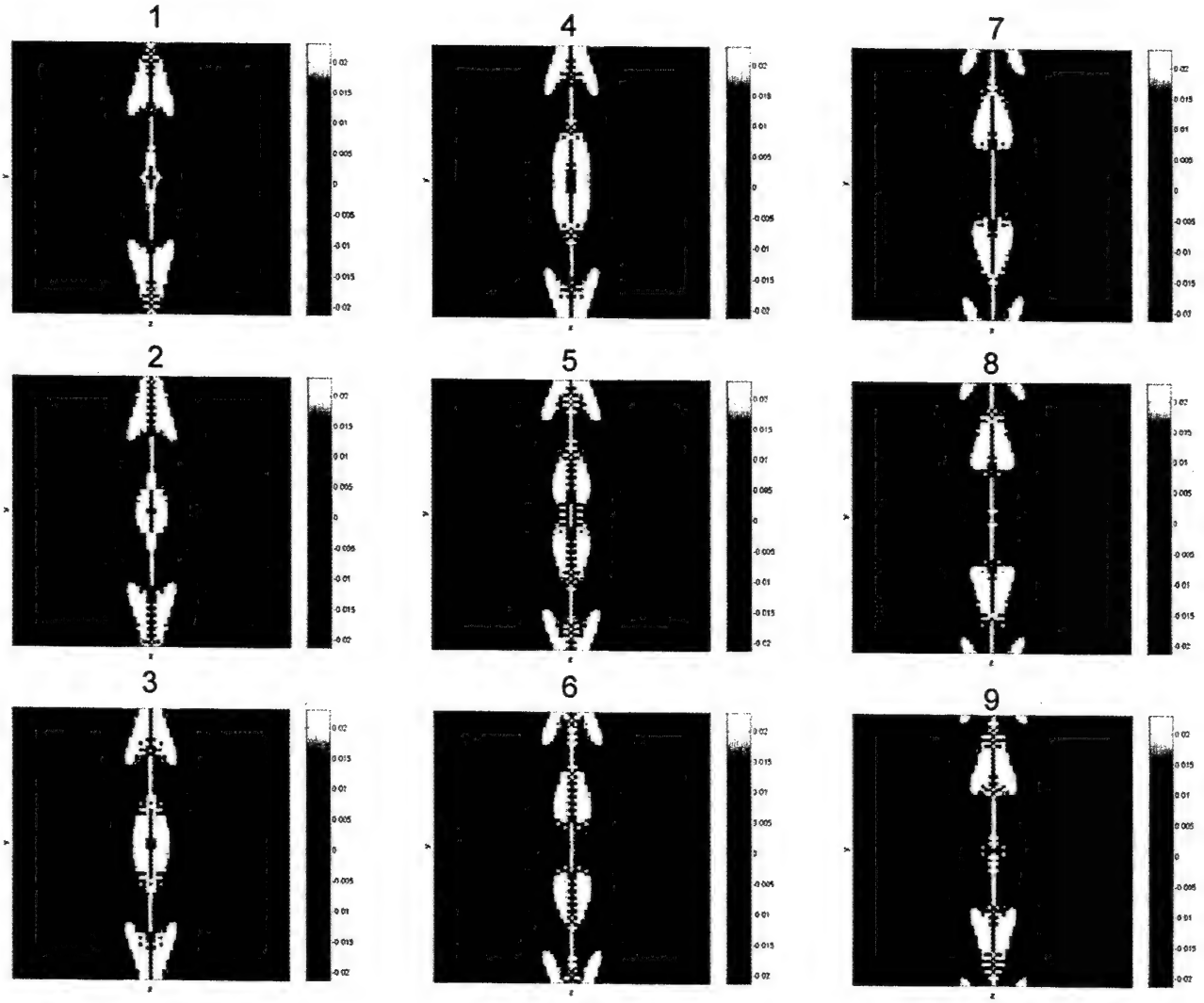

Figure 23. Ey field in Y-Z Plane. Propagation along Z.

B Antenna Input Impedance.

A second main Stanford goal has been to determine the first order effects of the dipole antenna plasma sheath on the antenna input impedance and to devise methods to control these effects. In this study we have used numerical solutions to the combined Poisson's and Lorentz's equations to determine the sheath characteristics in two dimensions. We treat each antenna element as an infinitely long cylinder and determine the sheath capacitance per meter of antenna length. Our approach is similar to that of *LaFramboise and Sonmor* [1993]

Working from our 2-D model, we have discovered a new method of controlling both the sheath dimensions and the sheath capacitance when the antenna is used to radiate VLF waves in the magnetospheric plasma. This is an important topic since the sheath capacitance is responsible for a large portion of the antenna input impedance.

To illustrate the new control method, we first show in Figure 26 the predictions of our 2-D model for the sheath radius r as a function of applied antenna potential. It can be seen that the sheath radius varies from a few centimeters for no applied voltage up to a few meters at 1000 Volts. This is roughly the range of voltages that would be applied to the dipole antenna during normal transmitting operations.

Since the sheath capacitance is a function of r, we can expect similar variations in the sheath capacitance as the applied voltage is varied. Figure 27 shows the predicted sheath capacitance as a function of r for a long dipole antenna. It varies widely from approximately 25 pF/m at low applied voltage to approximately 5 pF/m in the kV range.

For a long dipole antenna, the sheath capacitance is responsible for a major part of the input impedance of the antenna. However if we drive the antenna with a sinusoidal voltage of roughly 1000 V it is clear that the sheath capacitance will vary greatly during an RF cycle. Thus it is not possible to define an input impedance in a normal sense for the antenna. This is a major problem. If the antenna cannot be tuned, the radiation efficiency of the spacecraft VLF transmitting system will be very low and mission success will be compromised.

Using our 2-D sheath model, we have discovered that the problems inherent in a widely varying sheath capacitance can be mitigated by applying a DC bias to both elements of the dipole antenna. The bias can be either positive or negative. A large positive bias voltage can be applied

using a power source and an electron gun on the spacecraft. Negative current carried to the antenna by electrons is collected and expelled from the spacecraft using the power source and an electron gun. The maximum amount of bias achievable through this method, or similar methods, will be a subject for future study.

To illustrate the concept, we assume that a positive DC voltage bias of 5000 V is applied to both halves of a dipole antenna and the AC voltage is then swept from -2000 V to + 2000 V about the bias voltage. Results from our 2-D sheath model are shown in Figure 28. The Figure shows the sheath capacitance as a function of the sweeping voltage. It can be seen that the sheath capacitance varies only by approximately 10% over the 4000 V sweep range. These results suggest that this biasing technique can be very effective in controlling the dipole sheath capacitance.

For a positive bias of 5000 V, our 2-D model predicts that the electron current to the antenna would be approximately 20 microAmps/m. Thus a 100 m tip-to-tip dipole would draw about 2 mA, and the electron gun system would expend about 10 W in removing the arriving negative charge from the antenna. In addition there would be some power necessary to run the electron gun. The use of an ion gun along with a large negative bias might also be effective. The ion current arriving at the negatively biased antenna would be much smaller than the electron current expected for a positive bias of the same magnitude. Thus the power expended by the ion gun system in removing the arriving positive charge would be smaller, but more energy might be required to expel the ions from the ion gun because of their larger mass. There are clearly a number of questions that need to be addressed concerning this biasing technique. Nevertheless this method appears very promising.

In the coming three year period we propose to determine the feasibility of using high power electron or ion guns on the transmitting spacecraft to stabilize the sheath capacitance and allow straightforward tuning of the dipole antenna. We will also examine the possibility of using an active tuning network that compensates in real time for the sheath capacitance variation during each RF cycle.

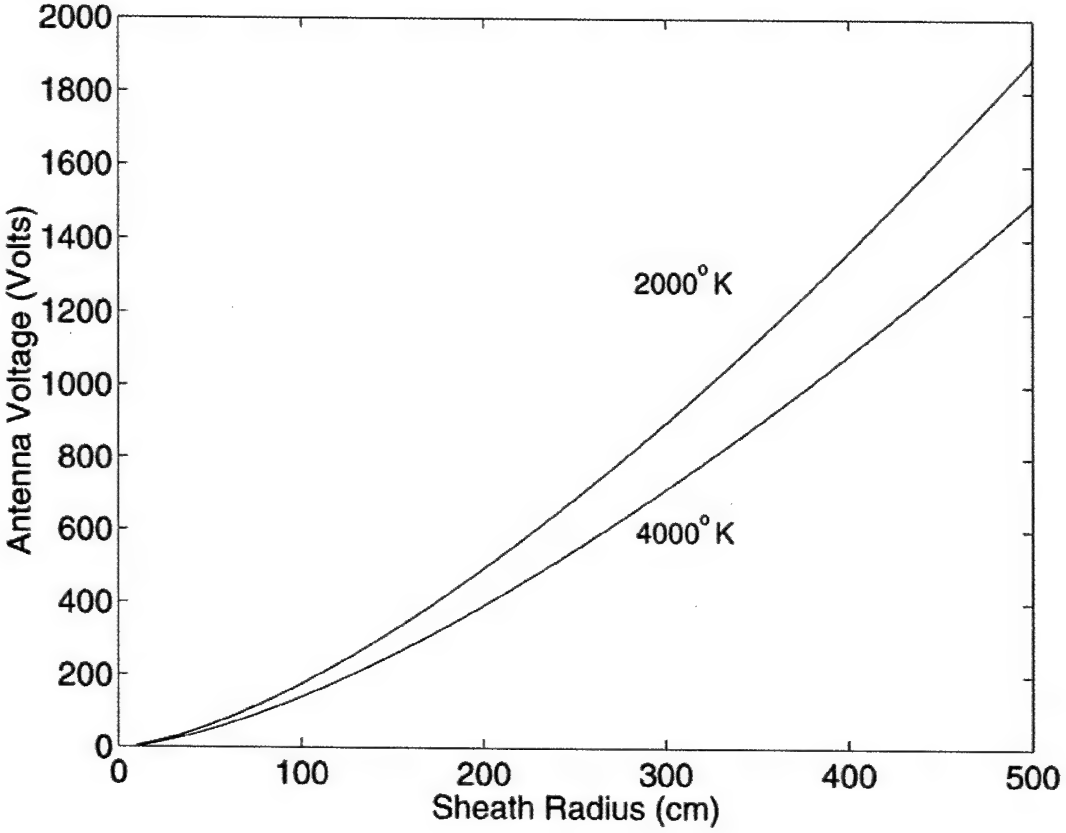

Figure 24. Antenna voltage and resultant plasma sheath radius for two values of plasma temperature.

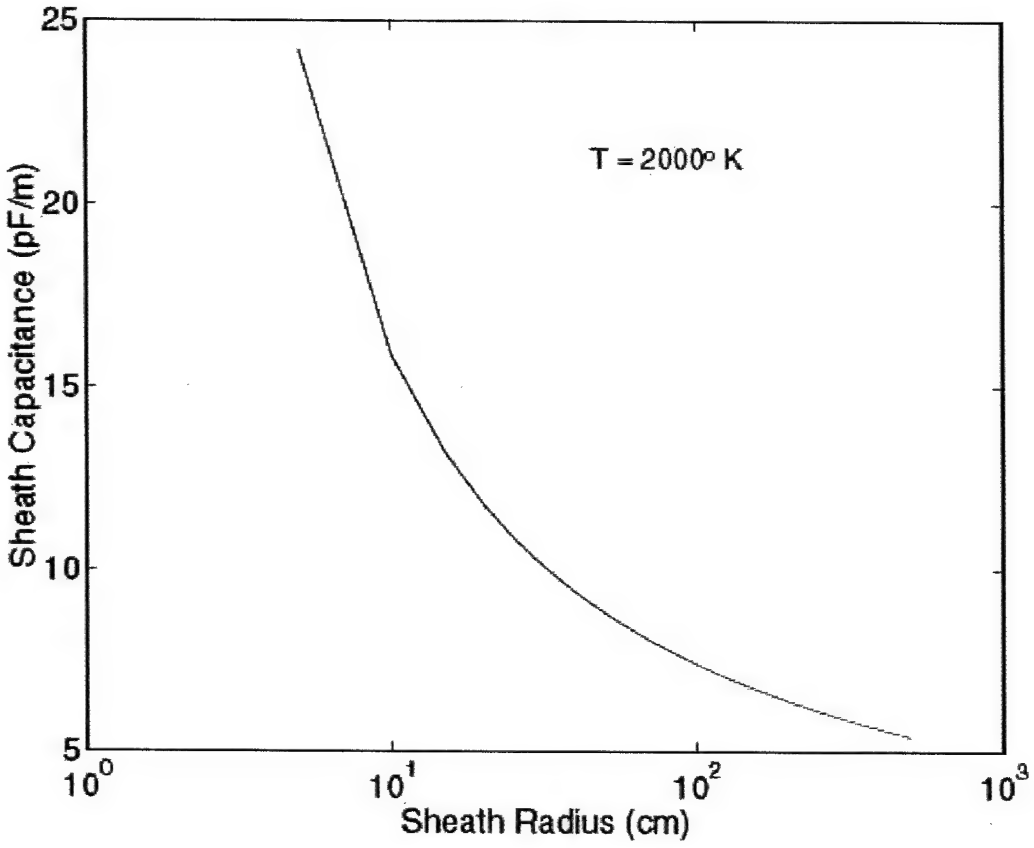

Figure 25. Sheath capacitance as a function of sheath radius.

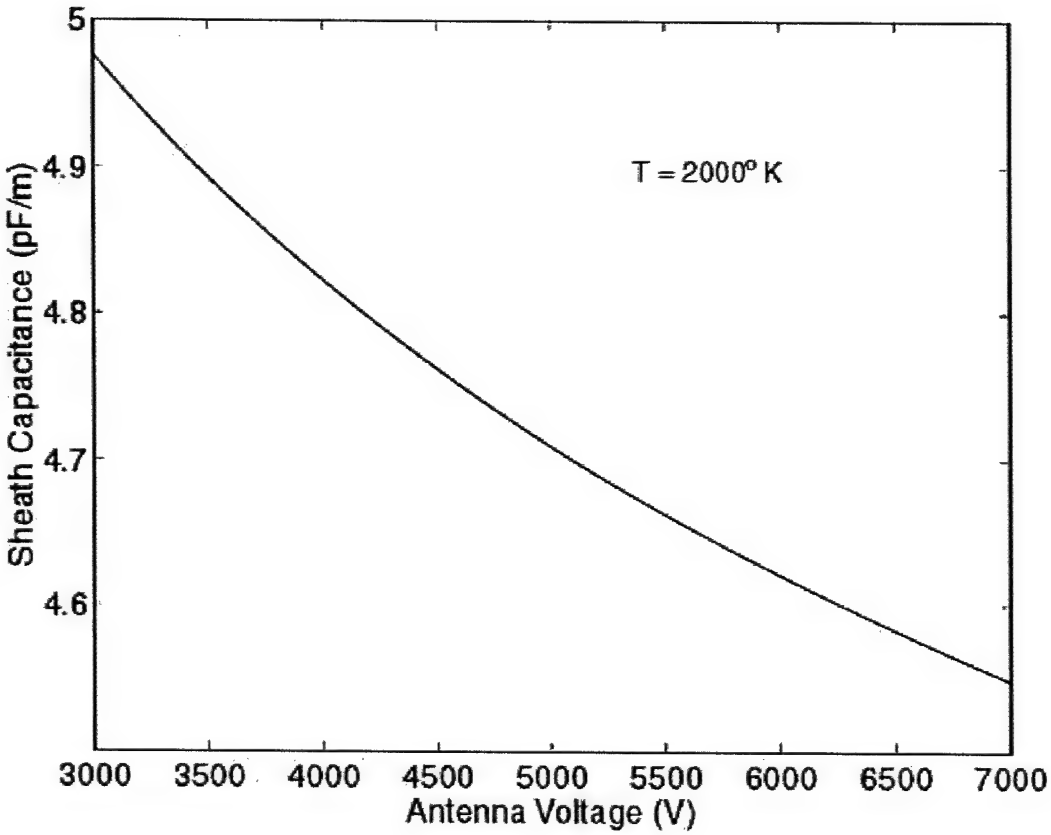

Figure 26. Sheath capacitance as a function of antenna voltage for a positive bias voltage of 5000 V.

C. Other Accomplishments

Additional goals of the Stanford effort have been: 1) the determination of nominal antenna requirements from wave-particle interaction models that are required to maximize particle decay rates for targeted populations, 2) the determination of the effects of Landau damping on the waves radiated from the antenna, 3) the determination of the energetic electron precipitation due to magnetospherically reflected whistlers, 4) the development .of a global overview of the total radiated VLF power from space necessary to match the effects of presently operating ground based VLF transmitters, and 5) the determination of the VLF input impedance of .large loop antennas in the magnetosphere. All of these topics must be considered when evaluating the feasibility of radiation belt control using space based VLF transmitting systems.

C.1. Antenna Length

For a variety of spacecraft orbits, we have determined the optimum dipole antenna length for maximizing the radiation of ELF/VLF waves with the correct wave normal angles for precipitating target electrons in the 1-10 Mev energy range. This work is reported in [*Inan et al. ,2002*].

C 2. Landau Damping

We have used data from the POLAR spacecraft to determine the characteristics of energetic electrons in the 100 eV - 2 keV energy range within the radiation belts. These characteristics were then used to assess the Landau damping that would affect the amplitude of the radiated ELF/VLF waves as they propagated through the belts. Knowledge of this damping and its variation with wave normal angle is critical in the evaluation of the feasibility of the mission. This work is reported in [*Bell, et al.,* 2002.]

C.3. Particle Precipitation by Magnetospherically Reflected Whistlers

Using Landau damping rates from the foregoing study, we have determined the energetic electron precipitation that is produced by magnetospherically reflected whistlers. This precipitation mode is one which we can emulate using spacebased ELF/VLF transmitters.[*Bortnik et al.*, 2002].

C.4. Global Overview

We worked with Tony Tether of ARPA to provide a global overview of the number, placement , and radiated power of a fleet of ELF/VLF radiating spacecraft which would be required to precipitate energetic electron fluxes equal to those presently being precipitated by ground based VLF transmitters. This work is reported in [*Inan et al.*, 2002]

C.5. The VLF Input Impedance of Large Loop Antennas

We determined the ELF/VLF radiation characteristics of large (100 m radius) loop antennas deployed from spacecraft in both low and high altitude orbits. In general, loops used for radiating VLF waves must be roughly of this size in order to radiate sufficient power. This type of antenna would appear to have an important advantage over dipole antennas in low Earth orbit, since a loop antenna with constant current does not develop a large plasma sheath that would affect its input impedance. However our results suggest that even small spatial variations of current around the loop can greatly affect the input impedance. This work is reported in [*Bell et al.*, 2002].

D. Joint Work

During the duration of his Grant we have worked jointly on various topics with AFRL/VSB personnel. Our work with Dr. J. Albert has led to the presentation of a joint paper at the Fall 2001 AGU meeting on: "Optimal VLF wave parameters for pitch angle scattering of trapped electrons" and to the submission of a joint paper to the Journal of Geophysical Research concerning controlled precipitation of radiation belt particles [Inan, et al., 2002].

References

Anile, A. M., N. Nikiforakis, and R. M. Pidatella, Assessment of a High Resolution Centered Scheme for the Solution of Hydrodynamical Semiconductor Equations, *Siam J. Sci. Comput. Vol. 22,* no. 5, pp. 1533-1548. (2000).

Bell,T. F., U. S. Inan, J. Bortnik, and J. Scudder, The Landau damping of magnetospherically reflected whistlers within the plasmasphere, *Geophys. Res. Lett.,* in press, 2002.

Bell, T. F., and U. S. Inan, The input impedance of large loop antennas at ELF/VLF frequencies in the magnetosphere, in preparation for *Radio Sci.* March, 2003.

Berenger, J. P., A Perfectly Matched Layer for the Absorption of Electromagnetic Waves, *Journal of Computational Physics, vol. 114*, pp 195-200, 1994.

Bortnik, J., U. S. Inan, and T. F. Bell, L-Dependence of energetic electron precipitation driven by magnetospherically reflecting whistler waves, *J. Geophys. Res.*, in press, June, 2002.

Hesthaven, J. S., The Analysis and Construction of Perfectly Matched Layers for the Linearized Euler Equations, ICASE 25th Anniversery, NASA/CR-201744 ICASE Report no. 97-49 September 1997.

Hockney, R. W., and J.W. Eastwood, *Computer Simulation Using Particles*, McGraw-Hill, New York, 1981.

Inan, U. S., T. F. Bell, J. Bortnik, and J. M. Albert, Controlled precipitation of radiation belt particles, submitted to *J. Geophys. Res.*, June, 2002.

Kurganov, A., and E. Tadmor, New High-Resolution Central Schemes for Nonlinear Conservation Laws and Convection-Diffusion Equations, *Jour. Comp. Phys, 160*, 241-282, 2000.

LaFramboise, J. G., and L. J. Sonmor, Current collection by probes and electrodes in space magnetoplasmas: A review, *J. Geophys. Res., 98*, 337, 1993.

Lee, J. H., and D. K. Kalluri, Three-Dimensional FDTD Simulation of Electromagnetic Wave Transformation in a Dynamic Inhomogeneous Magnetized Plasma, *IEEE Trans. Antennas Propagation, vol.47*, no. 7, pp. 1146-1151, July. 1999.

Lymberopoulos, D. P., and D. J. Economou, Two-Dimensional Self-Consistant Radio Frequency Plasma Simulations Relevant to the Gaseous Electronics Conference RF Reference Cell, *Jour. Research. Nat. Inst. Standards and Technology. Vol. 100,* no. 4, pp 473-494, August 1995.

Meezan, N. B., and M. A. Cappelli, A Kinetic Study of Electron-Wall Collisions in a Hall Thruster, 27th International Electric Propulsion Conference, Pasadena, CA., October, 2001.

Ordonez, C. A., Boundary Conditions Including Sheath Effects at a Plasma-facing Surface, *Physical Rev. E, vol. 55*, no. 2, pp. 1858-1871, February 1997.

Roden, J. A., and S. D. Gedney, Convolutional PML (CPML): An Efficient FDTD Implementation of the CFS-PML for Arbitrary Media, Submitted to *Microwave and Optical Technology Letters,* June, 2000.

Sheridan, T. E., and. J. Goree, Collisional Plasma Sheath Model, *Phys. Fluids B, vol. 3*, no. 10, October, 1991.

Taflove, A., and S. C. Hagness, *Computational Electrodynamics: The Finite-Difference Time-Domain Method, 2nd ed.*, Artech House, Norwood, MA, 2000.

Young, J. L., A Full Finite Difference Time Domain Implementation for Radio Wave Propagation in a Plasma, *Radio Sci., Vol. 29*, no. 6, pp. 1513-1522. Nov-Dec 1994.

Young, J. L., and F. P. Brueckner, A Time Domain Numerical Model of a Warm Plasma, *Radio Science. Vol. 29*, no. 2, pp. 451-463. Mar-April 1994.